Canadian Journal of
Fisheries and
Aquatic Sciences

Article

Spatially varying effects of the California Undercurrent on Pacific hake distribution

Michael J. Malick[a], **Mary E. Hunsicker**[b], **Melissa A. Haltuch**[c], **Sandra L. Parker-Stetter**[d], **Kristin N. Marshall**[e], **John E. Pohl**[e], **Aaron M. Berger**[f], **Samantha A. Siedlecki**[g], **Stéphane Gauthier**[h,i], **and Albert J. Hermann**[j]

[a]Environmental and Fisheries Sciences Division, Northwest Fisheries Science Center, National Marine Fisheries Service, National Oceanic and Atmospheric Administration, Port Orchard, WA 98366, USA; [b]Fish Ecology Division, Northwest Fisheries Science Center, National Marine Fisheries Service, National Oceanic and Atmospheric Administration, Newport, OR 97365, USA; [c]Resource Ecology and Fisheries Management Division, Alaska Fisheries Science Center, National Marine Fisheries Service, National Oceanic and Atmospheric Administration, Seattle, WA 98115, USA; [d]Resource Assessment and Conservation Engineering Division, Alaska Fisheries Science Center, National Marine Fisheries Service, National Oceanic and Atmospheric Administration, Seattle, WA 98115, USA; [e]Fishery Resource Analysis and Monitoring Division, Northwest Fisheries Science Center, National Marine Fisheries Service, National Oceanic and Atmospheric Administration, Seattle, WA 98112, USA; [f]Fishery Resource Analysis and Monitoring Division, Northwest Fisheries Science Center, National Marine Fisheries Service, National Oceanic and Atmospheric Administration, Newport, OR 97365, USA; [g]Department of Marine Sciences, University of Connecticut, Groton, CT 06340, USA; [h]Institute of Ocean Sciences, Fisheries and Oceans Canada, Sidney, BC V8L 4B2, Canada; [i]Department of Biology, University of Victoria, Victoria, BC, Canada; [j]Cooperative Institute for Climate, Ocean, and Ecosystem Studies, University of Washington, Seattle, WA 98105, USA

Corresponding author: **Michael J. Malick** (email: michael.malick@noaa.gov)

Abstract

In the California Current Ecosystem, the California Undercurrent (CU) is the predominate subsurface current that transports nutrient-rich water from southern California poleward. In this study, we used a large dataset of spatially explicit in situ observations of Pacific hake (*Merluccius productus*) and the CU (36.5–48.3°N) to estimate relationships between northward undercurrent velocity and hake distribution and determine whether these relationships vary across space or life-history stage. We found that both hake occurrence and density had strong spatially complex relationships with the CU. In areas north of 44°N (central Oregon), the CU effect was spatially consistent and opposite for occurrence (negative) and density (positive), indicating that hake may aggregate in areas of high northward velocity in this region. In areas south of 44°N, the CU effect showed a cross-shelf gradient for both occurrence and density, indicating a more nearshore hake distribution when northward velocity is higher in this region. Together, our results suggest that future changes in the CU due to climate change are likely to impact hake differently in northern and southern areas.

Key words: Pacific hake, California Undercurrent, ocean currents, transport, nonstationary

Introduction

Conditions in coastal marine ecosystems are rapidly emerging from the historical envelope of variability, driven by anthropogenic climate warming (Henson et al. 2017; Laufkötter et al. 2020). Gradual shifts in mean physical ocean conditions and more frequent extreme events can impact higher-trophic-level species via multiple pathways. In eastern boundary systems, vertical transport and horizontal transport represent alternative pathways that redistribute nutrients and lower-trophic-level organisms, which can affect the distribution or productivity of marine fish populations (Rykaczewski and Checkley 2008; Di Lorenzo et al. 2013). For example, in the northern region of the California Current Ecosystem (CCE), variability in horizontal ocean transport contributes to shifting zooplankton assemblages, which are important food resources for marine and anadromous fish species (Keister et al. 2011; Malick et al. 2017).

Impacts of abrupt or gradual changes in ecosystem conditions are particularly concerning for migratory species if the changes alter migration routes or shift distributions out of alignment with established fisheries management boundaries (Pinsky et al. 2018). In the CCE, Pacific hake (*Merluccius productus*; hereafter just hake) is the most abundant groundfish species and supports one of the largest transboundary commercial fisheries in the U.S. (NOAA 2017). Hake migrate each spring from spawning grounds off the southern U.S. West Coast to more northern feeding grounds off the northern U.S. West Coast and British Columbia, Canada, occasionally migrating as far north as Southeast Alaska (Ressler et al. 2007). The proportion of the hake stock that migrates into Canadian waters, however, is variable across years. For example, in 1998 the hake stock ranged from southern California to Southeast Alaska and was centered near Vancouver Island, whereas in 2001 disproportionately less hake were observed

Table 1. Summary of survey data used for analysis.

Year	Start	End	N transects	N hake	% absent	N $v_{100-300}$	CoG
1995	13 July	15 August	72	3808	40.3	6936	42.6
1998	9 July	11 August	74	4304	55.0	7802	44.4
2001	19 June	18 July	70	3731	70.5	5154	41.5
2009	2 July	13 August	71	3630	81.0	6812	44.8
2017	29 June	17 August	62	3928	69.1	7551	40.7
2019	24 June	15 August	63	4057	56.2	9358	42.6

Note: Start gives the date the survey started at 36.5°N; end gives the date the survey reached 48°N; N transects gives the number of survey transects; N hake gives the number of binned (0.5 nmi (1 nmi = 1.852 km)) hake observations that had a corresponding undercurrent observation; % absent gives the percentage of hake observations (N hake column) that had zero biomass; N $v_{100-300}$ gives the total number of velocity observations at 100–300 m depth (includes undercurrent observations not matched to a hake observation); CoG gives the center of gravity of the hake stock along the U.S. West Coast.

in Canadian waters (Malick et al. 2020*a*). This variability in the proportion of the hake stock in Canada has important consequences for the hake fishery where a key part of management is the allocation of catch between countries.

Recent work suggests that climate change-induced shifts in the migration pattern of hake could have negative consequences for the management of the international Pacific hake fishery (Jacobsen et al. 2022). Indeed, hake are believed to be distributed, in part, by responses to physical and biological cues that vary seasonally and inter-annually (Ressler et al. 2007). In particular, processes that aggregate or transport prey resources or assist in migration, such as subsurface currents, have been hypothesized as key drivers of hake distribution (Bakun 1996; Mackas et al. 2001). Circulation in the CCE is dominated by two currents, the surface oriented and equatorward flowing California Current and the subsurface poleward flowing California Undercurrent (CU) (Hickey and Banas 2008). The CU starts near Baja California and flows northward to Vancouver Island, transporting nutrient-rich water that contributes to the high productivity of the CCE (Thomson and Krassovski 2010, 2015). The CU exhibits strong cross-shelf and latitudinal gradients; the core of the CU (>0.1 $m \cdot s^{-1}$) occurs at depths of 200–275 m and 20–25 km off the shelf break (Pierce et al. 2000) and current strength tends to attenuate with increasing latitude (Garfield et al. 1999; Pierce et al. 2000; Connolly et al. 2014).

The CU could impact hake distribution either through assisting hake migration or via the distribution of prey resources (Agostini et al. 2006, 2008). Previous research has indicated a moderately strong relationship between hake distribution and the CU, although this research was limited to a narrow geographical region (38–43°N) and 2 years of data (Agostini et al. 2008). Spatial complexity in the CU across the CCE further suggests that the degree to which subsurface transport impacts hake distribution may vary across space or life-history stage (Ciannelli et al. 2012; Li et al. 2018). The effects of the CU on hake distribution may be more acute for younger hake, which are distributed further south than older hake, corresponding to the region where the CU has a stronger poleward flow (Malick et al. 2020*a*). Similarly, younger hake prefer less mobile prey items compared to older conspecifics and the CU may therefore have a stronger impact on the distribution of these prey items (Livingston and Bailey 1985; Buckley and Livingston 1997). The cross-shelf and latitudinal gradients observed in the strength of the CU could also result in a spatially complex relationship with hake distribution, e.g., through threshold effects associated with the attenuation of the CU strength with latitude.

In this study, we used a new multiyear coastwide dataset of hake biomass and undercurrent velocities to evaluate the functional form of the relationship between hake distribution (both occurrence and density) and the CU. In particular, we had three research objectives: (1) characterize interannual variability in the CU during the summer period when hake are broadly distributed across the CCE, (2) determine whether the CU can explain variability in the distribution of hake along the U.S. West Coast, and (3) determine whether relationships between hake distribution and the CU vary across space or life-history stage. Combined, these objectives allowed us to gain insights into the drivers of hake distribution and help reduce uncertainties about the extent of northward migration, which helps inform management and survey planning decisions.

Methods

Pacific hake data

The coastal hake stock is monitored jointly by a United States and Canada summer integrated ecosystem assessment and Pacific hake acoustic-trawl survey. Surveys were conducted triennially before 2002 and biennially after 2002, with an additional survey in 2012. Surveys aim to sample the entire hake distribution, typically starting near Monterey Bay, California and moving northward along the coast up to Dixon Entrance or until hake are no longer observed (usually around 54.5°N; see Malick et al. 2020*a*). The spatial extent of the data analyzed here, however, was limited to the U.S. West Coast (36.5–48.3°N) because concurrent ship-borne undercurrent data were not available in more northern areas. The southern starting point of the hake survey varied across years; therefore, we limited the southern extent to the northernmost starting point of a survey across all years included in the analysis (36.5°N) to ensure multiple years of data were available at each latitude. In total, hake biomass and undercurrent data with sufficient spatial coverage were available for six survey years (Table 1).

Surveys were conducted between June and August each year with the surveys generally starting near the end of June and reaching 48°N around mid-August (Table 1). The exception was 2001, where the survey timing was shifted approximately 2 weeks earlier. The number of transects within the

study domain was fairly consistent across years ranging between 62 in 2017 and 74 in 1998 (Table 1).

Acoustic backscatter measurements were collected continuously throughout the survey at 38 kHz and were converted to hake biomass estimates using the methods outlined in Fleischer et al. (2008) and Malick et al. (2020*a*). When paired with trawl samples of age composition, age-specific (ages 2–20) biomass estimates were available for 0.926 km (0.5 nmi (1 nmi = 1.852 km)) bins along each transect.Age-specific biomass estimates were only produced for age-2 and older hake because of difficulties in sampling age-1 hake. We further grouped the data into three age groups that correspond to life-history stages that have previously been shown to have different responses to physical ocean conditions: age 2, which are immature hake, ages 3–4, which represent a mixture of immature and mature hake, and age 5+, which represent mature hake (Malick et al. 2020a). To produce a presence/absence dataset, we coded bins with nonzero biomass as hake occurrences and bins with zero biomass as hake absences.

Finally, to summarize the north–south distribution of the hake stock, we calculated the latitudinal center of gravity for each age group and for all ages combined by taking the mean latitude of hake observations weighted by the biomass found at each location.

California Undercurrent data

CU velocity was derived from a hull-mounted acoustic Doppler current profiler (ADCP; Teledyne RD instruments). Across the study period, CU data were collected using two different ADCP units. Prior to 2010, a four-transducer-faced 150 kHz Janus configuration was used, whereas later surveys used a 75 kHz flat phased-array single transducer that generated all four beams simultaneously. The two instruments could reliably measure ocean currents from the surface down to at least 300 m.

To avoid interference between the ships' transducers, each ADCP pulse was run in narrow-band mode and synchronized to fire in coordination with the scientific echosounders used for measuring acoustic hake backscatter. We used a vertical bin width of 8 m. Ensemble averaging times prior to 2010 varied slightly across collections, from 2.5 to 5 min, whereas later ensemble averaging collections were 5 min.

Undercurrent data before 2010 were postprocessed using CODAS and later data (2010 and later) were postprocessed using the software UHDAS, which is based on CODAS (https://currents.soest.hawaii.edu/docs/adcp_doc/index.html). ADCP postprocessing generally followed the methods outlined in Pierce et al. (2000). Briefly, postprocessing consisted of three main steps: (1) using standard diagnostics to determine the necessary heading correction for differences between the linked POSMV and gyro, and to account for differences in location between the ship's GPS antenna and the ADCP; (2) calibration of the phase and amplitude error between the ship velocity and subsurface currents; and (3) velocity smoothing of the reference layer. The postprocessing resulted in earth-referenced water column profiles of velocities north and east along survey transects.

Table 2. Alternative model structures used in the analysis.

Model	Structure
M1	$z_{i,t} = \alpha + a_i + g_1(\text{lon}_i, \text{lat}_i)$
M2	$z_{i,t} = \alpha + a_i + g_1(\text{lon}_i, \text{lat}_i) + s(v_{i,t})$
M3	$z_{i,t} = \alpha + a_i + g_1(\text{lon}_i, \text{lat}_i) + g_2(\text{lon}_i, \text{lat}_i) \cdot v_{i,t}$

Note: Each model was fit independently to the occurrence and biomass datasets. In each equation, $z_{i,t}$ is either the logit transformed probability of occurrence (occurrence models) or the natural log of expected hake biomass conditional on presence (biomass models). See the "Methods" section for equation term definitions.

Previous research has indicated the core of the undercurrent occurs at depths of 200–275 m but varies between 100 and 300 m, which corresponds to depth preferences of hake (Pierce et al. 2000; Ressler et al. 2007). Therefore, to characterize the strength of the CU at a particular location, we averaged each north velocity water column profile over the depths of 100–300 m (inclusive), only using water column velocity profiles that had at least three velocity values across depth of 100–300 m. We then assigned each hake observation the depth-averaged north velocity value that was closest (based on Euclidean distance) within a year and excluded hake observations that did not have a velocity value within 3 km (median distance was 0.37 km).

Statistical models

We used generalized additive models (GAM) to estimate the effects of the northward velocity component of the undercurrent on hake occurrence and biomass distribution (Ciannelli et al. 2012; Brodie et al. 2019). The occurrence model was a binomial GAM with a logit link, whereas the biomass model had a normal error distribution. The occurrence and biomass models were fit independently; however, both models had the same general form

$$z_{i,t} = \alpha + a_t + g(\text{lon}_i, \text{lat}_i) + f(v_{i,t}) + \epsilon_{i,t}$$

where $z_{i,t}$ is either the logit-transformed probability of occurrence (occurrence model) or the natural log of expected hake biomass conditional on presence (biomass model) at location i in year t, α is the intercept, a_t is a random year effect assumed to be normally distributed with mean 0 and variance σ_a^2, g is a bivariate smooth function of longitude (lon) and latitude (lat), f is a smooth function describing the effect of the undercurrent (v), and ϵ are model residuals.

We used GAM models for both the occurrence and biomass models because of previous evidence that has shown nonlinear and spatially varying environmental effects on hake occurrence and biomass (Malick et al. 2020*a*, 2020*b*). For both the occurrence and biomass models, we evaluated two alternative functional forms of the undercurrent effect, f. First, we assumed that the effect was nonlinear and the same at all locations (i.e., spatially stationary). In this form, f was defined as a univariate smooth function to allow for nonlinear relationships, i.e., $s(v_{i,t})$ (model M2, Table 2). Second, we allowed the undercurrent effect to vary across space. In this spatially varying form, f was defined as the product of bivariate smoothing of lon and lat and the undercurrent covariate, i.e., $g(\text{lon}_i, \text{lat}_i) \cdot v_{i,t}$; i.e., the undercurrent effect is assumed to

Fig. 1. Summary of undercurrent velocities averaged over 100–300 m. (A) Histogram of undercurrent velocity (m·s $^{-1}$); dot and range line below histogram give the median (dot) and the inter-quartile range, respectively. (B) Annual median (dots) and inter-quartile range (vertical lines) of undercurrent velocity. (C) Map of mean velocity across all years, data are averaged into 15 km grid cells and grey line shows the 200 m isobath. Base map and bathymetric data are from http://www.naturalearthdata.com. Map is drawn in Universal Transverse Mercator (UTM) coordinates referenced to the WGS84 geographic coordinate system.

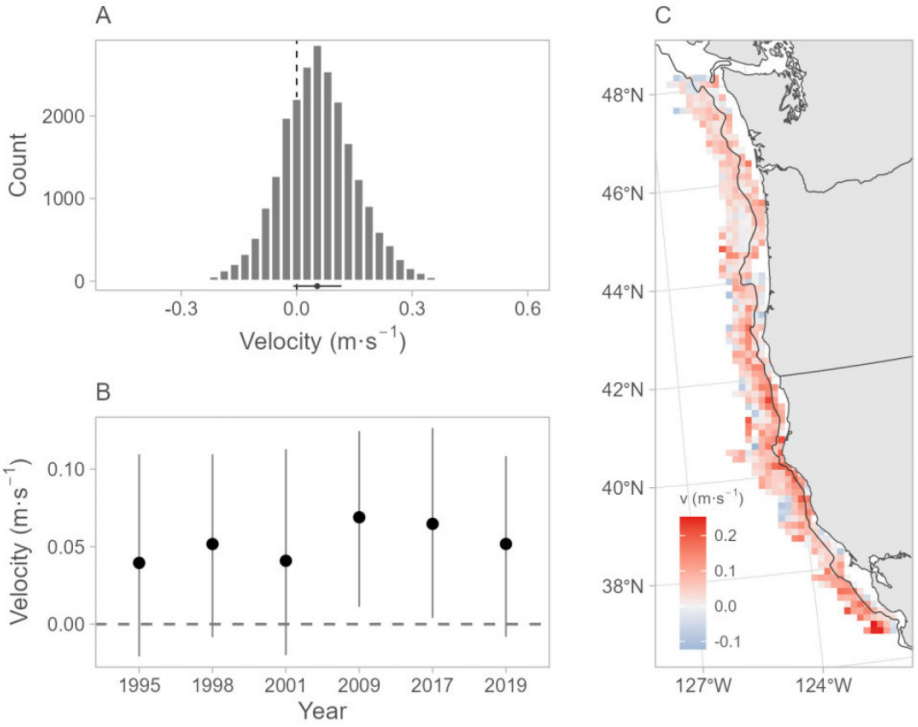

be locally linear, but can vary smoothly across space (model M3, Table 2). To help understand the relative importance of the undercurrent covariates in explaining variability in hake occurrence and biomass, we also fit the simpler model that excluded the undercurrent effect (model M1, Table 2). Because previous research has indicated physical ocean conditions can have age group-specific effects on hake, we further evaluated the effects of the undercurrent on three age groups of hake (i.e., age 2, ages 3–4, and age 5+) by fitting each of the three models separately for each age group (Malick et al. 2020a).

Univariate and bivariate smooths were constructed using thin plate regression splines (Wood 2003). Models were fit via restricted maximum likelihood using a standard mixed model parameterization (Wood 2011). Model fits were assessed using root mean squared error, deviance explained, examination of residuals, and for the occurrence models, the area under the curve. We compared models using Akaike information criterion (AIC). All analyses were conducted using R statistical software v4.1.2 and the mgcv package (Wood 2017; R Core Team 2019).

Results

Undercurrent velocities

Across all years, undercurrent velocity was primarily northward (72% of all observations) with an average velocity at 100–300 m of 0.056 m·s $^{-1}$ and a range of −0.445–0.602 m·s $^{-1}$ (Figs. 1 and S1). Annually, the percent of observations that had northward flow ranged from 78% in 2009 to 66% in 1995 and 2001. These years also exhibited the highest and lowest average velocities, 0.070 m·s $^{-1}$ in 2009 and 0.045 m·s $^{-1}$ in 2001.

Northward velocities in the southern portion of the study region (south of 44°N) were 2.2 times stronger compared to the northern area (north of 44°N) with an average velocity of 0.072 m·s $^{-1}$ in the south and 0.033 m·s $^{-1}$ in the north (Figs. 1 and S2). Velocities south of 44°N also exhibited a cross-shelf gradient with northward velocities being 1.5 times stronger at locations where bottom depth was less than 1000 m compared to deeper locations (Figs. 1 and S2). In the northern area, there was less evidence for a cross-shelf gradient with velocities tending to be slightly higher at nearshore locations with bottom depths less than 150 m (Fig. S2).

Hake occurrence and biomass

Hake were absent in 62% of observed locations across all years (Figs. 2 and S3). Annually, this ranged from a low of 40% in 1995 to a high of 81% in 2009 (Table 1). Hake were most often observed in locations just off the 200 m shelf break with bottom depths in the range of 200–500 m and also tended to have the highest densities in these locations (Figs. 2, S4, and S5). Average age-2 hake density was seven times higher in the southern region (south of 44°N), compared to the northern

Fig. 2. Mean log biomass across all years for all ages, age 2, ages 3–4, and age 5+ hake. Dark purple indicates locations where no hake were observed and brighter yellow indicates locations with high hake biomass. Data are averaged into 15 km grid cells and grey line shows the 200 m isobath. Base map and bathymetric data are from http://www.naturalearthdata.com. Maps are drawn in UTM coordinates referenced to the WGS84 geographic coordinate system.

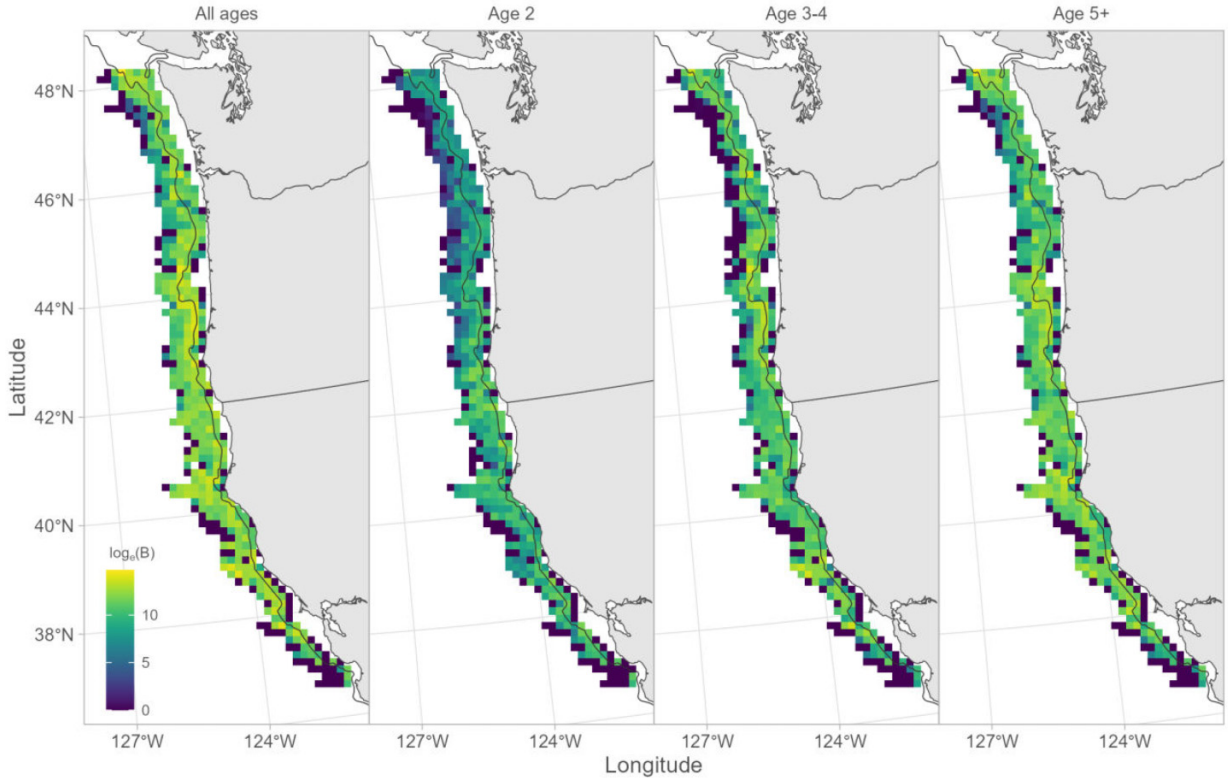

region (Fig. 2; mean biomass in north = 12.85 t; mean biomass in south = 94.02 t). In contrast, average densities for hake ages 3–4 and age 5+ were comparable in the northern and southern regions (Fig. 2).

Across all ages, the latitudinal center of gravity of hake distribution was not strongly correlated with mean annual undercurrent velocity ($r = 0.28$; Tables 1 and 3). Age group-specific correlations, however, revealed that the center of gravity of the age-2 group was strongly associated with average northward velocity ($r = 0.86$, $p = 0.028$), suggesting that the undercurrent may assist migration of smaller, immature hake (Table 3).

Table 3. Correlations between hake distribution latitudinal center of gravity for each age group and mean annual northward velocity at 100–300 m and associated 95% confidence intervals (CI).

Age	r	95% CI
All	0.28	−0.69, 0.89
Age 2	0.86	0.16, 0.98
Ages 3–4	0.20	−0.73, 0.87
Age 5+	0.32	−0.66, 0.90

Occurrence and biomass models

For both the occurrence and biomass models (combined ages and age group-specific models), the model that included the spatially varying undercurrent term had the most support according to AIC and the spatially varying term was statistically significant in all models (Tables 4, S1, and S2).

The spatially varying term in the combined-age occurrence model indicated a negative association between hake occurrence and northward velocity of the undercurrent in the northern part of the study region (north of 44°N) and a positive association in the southernmost part of the study region (south of 39°N) (Fig. 3A). In the intermediate latitudes (39–44°N), the relationship between the undercurrent and hake occurrence varied cross-shelf with nearshore areas having a positive relationship and offshore areas having a negative relationship (Fig. 3A). The spatially varying effect of the undercurrent on hake occurrence for both the age-2 and age-5+ models followed nearly identical patterns to the combined age model (Fig. 4). For ages 3–4 hake, however, the occurrence model indicated a slightly different pattern where there was a more consistent cross-shelf positive effect in the region 41–46°N, although the strongest positive correlations were still observed in nearshore areas.

The combined-age biomass model revealed that the spatially varying effect of the undercurrent on hake density was the opposite of the occurrence model in the northern and southernmost areas: a mostly positive effect in areas north

Table 4. Best fit model summaries.

Data	Age	Model	Dev. expl.	RMSE	EDF	AUC
Occurrence	All	M3	13.2	0.445	9.34∗	0.740
	Age 2	M3	14.9	0.431	9.33∗	0.755
	Ages 3–4	M3	14.0	0.426	9.24∗	0.752
	Age 5+	M3	13.3	0.444	9.34∗	0.742
Biomass	All	M3	22.3	1.660	7.60∗	–
	Age 2	M3	44.5	1.922	7.34∗	–
	Ages 3–4	M3	38.6	1.743	7.23∗	–
	Age 5+	M3	18.6	1.716	8.60∗	–

Note: The model column gives the model number from Table 2; dev. expl. gives the percent deviance explained; RMSE gives the root mean squared error; EDF gives the estimated degrees of freedom for the undercurrent velocity term; and AUC gives the estimated area under the curve for the occurrence models. ∗ indicates that model term was significant at $p < 0.05$.

Fig. 3. Marginal effects of the spatially varying velocity effect from models M3. Red locations indicate a positive linear effect of velocity on hake occurrence (panel A) or hake biomass (panel B) and blue indicates a negative effect. Stippling indicates locations where the effect was significantly different from zero. Grey line shows the 200 m isobath. Base map and bathymetric data are from http://www.naturalearthdata.com. Maps are drawn in UTM coordinates referenced to the WGS84 geographic coordinate system.

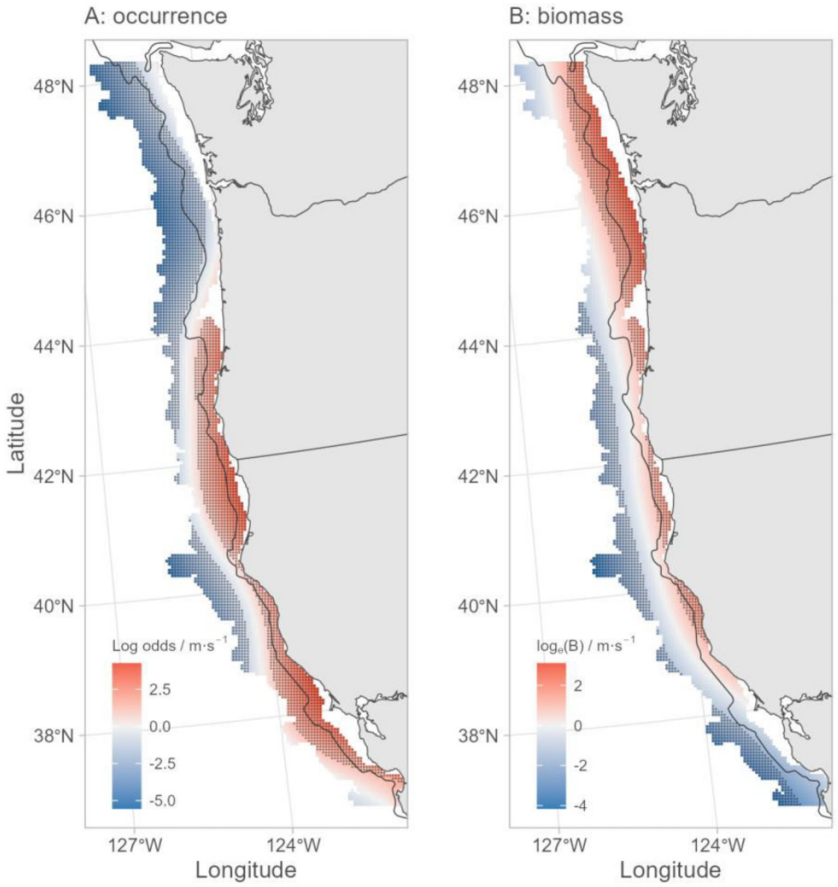

of 44°N and a strong negative effect in areas south of 39°N (Fig. 3B). The effects in the center of the study region, however, were similar with strong positive effects in nearshore areas and negative effects in offshore areas (Fig. 3B). The relationship between age-2 hake density and the undercurrent exhibited less cross-shelf variability compared to older age groups (Fig. 5). For age-2 hake, there tended to be a consistent positive association between density and the undercurrent in areas north of 44°N and a negative association in areas south of 44°N. In contrast, the ages 3–4 and age 5+ biomass models showed a strong cross-shelf gradient in the effects of the undercurrent on hake distribution that extended to the northernmost part of the study area (48.3°N).

Fig. 4. Age-specific marginal effects of the spatially varying velocity effect from hake occurrence model M3. Red locations indicate a positive linear effect of velocity on hake occurrence and blue indicates a negative effect. Stippling indicates locations where the effect was significantly different from zero. Grey line shows the 200 m isobath. Base map and bathymetric data are from http://www.naturalearthdata.com. Maps are drawn in UTM coordinates referenced to the WGS84 geographic coordinate system.

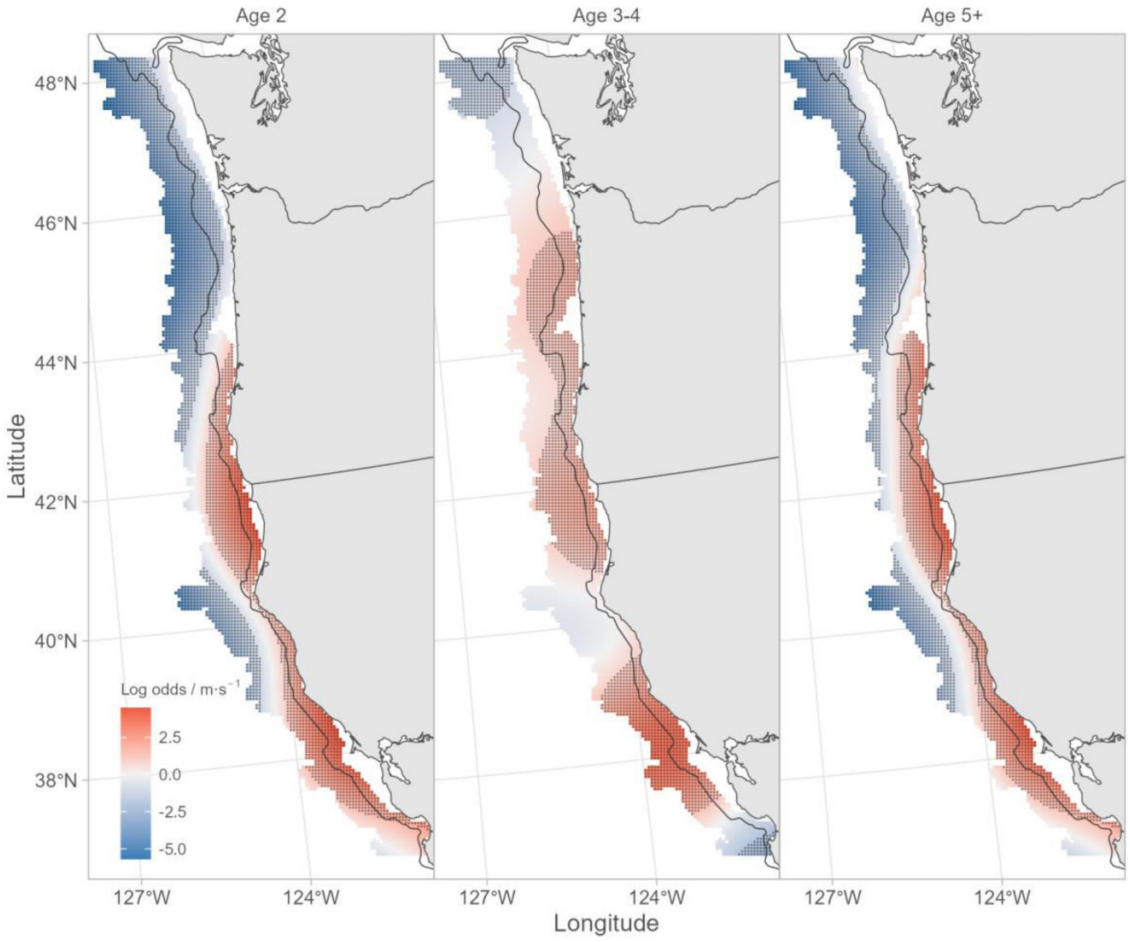

Discussion

In this study, we used in situ observations of hake and the CU to estimate relationships between northward undercurrent velocity and hake distribution. We found that (1) both hake habitat preferences and densities had strong spatially complex relationships with northward undercurrent velocity, (2) in areas north of 44°N, the CU effect tended to be spatially consistent and opposite for occurrence (negative) and density (positive), and (3) in southern areas, the CU effect showed a cross-shelf gradient for both occurrence and density (positive effect nearshore and negative effect offshore) with the northern extent of the gradient effect on hake density tending to be greater for older age groups. Together, these results suggest that hake occurrence and density distributions have spatially heterogeneous responses to environmental variability that also interact with internal stock dynamics (i.e., age composition).

Our results agree with previous findings by Agostini et al. (2006, 2008) by indicating that the CU is an important driver of hake distribution. There are two primary hypotheses linking variability in the CU to hake distribution. First, the CU may aggregate or transport prey resources that hake require. Hake have a diverse diet, yet two euphausiid species, *Euphausia pacifica* and *Thysanoessa spinifera*, have repeatedly been identified as key diet items during summer months (Livingston and Bailey 1985; Buckley and Livingston 1997; Miller et al. 2010). Euphausiids are widely distributed along the west coast of North America and their distribution has been linked to ocean conditions, including temperature and ocean currents (Mackas et al. 2001; Santora et al. 2011; Phillips et al. 2022). In the northern CCE, regional-scale zooplankton community composition is partly driven by ocean current patterns where more southern zooplankton species are advected into more northern areas during years with a stronger northward flow (Mackas et al. 2001; Peterson and Keister 2003; Keister et al. 2011). This suggests that hake may be responding to changes in prey availability that is subsequently impacted by the strength and location of ocean current patterns.

Second, a strong northward flow may assist hake in their summer northward migration, particularly for smaller hake, where a stronger northward undercurrent could reduce

Fig. 5. Age-specific marginal effects of the spatially varying velocity effect from hake biomass model M3. Red locations indicate a positive linear effect of velocity on hake biomass and blue indicates a negative effect. Stippling indicates locations where the effect was significantly different from zero. Grey line shows the 200 m isobath. Base map and bathymetric data are from http://www.naturalearthdata.com. Maps are drawn in UTM coordinates referenced to the WGS84 geographic coordinate system.

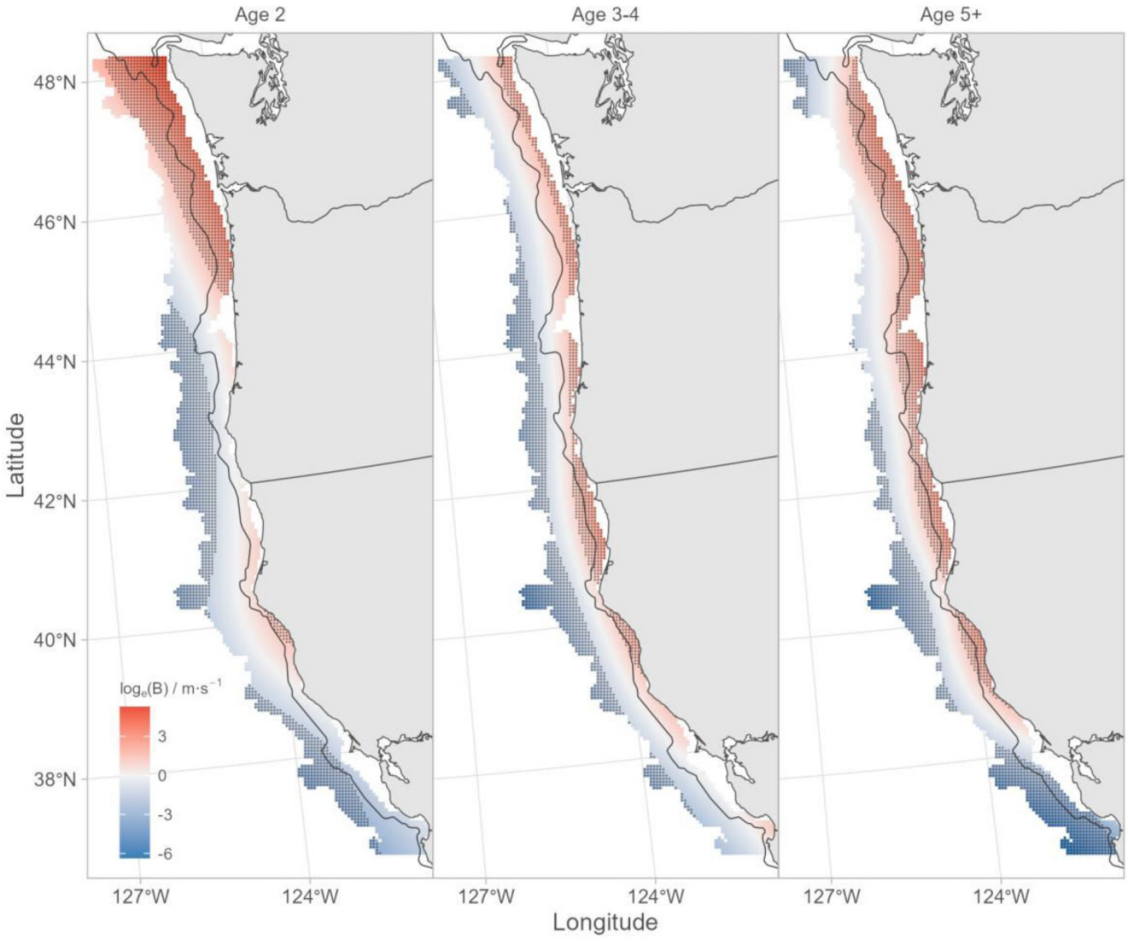

energy expenditure during the migration. This may be particularly important in the southern portion of the study area where the undercurrent is the strongest and age-2 hake tend to be most prevalent. Although the degree to which ocean currents may assist pelagic fish migration is poorly understood, other marine species such as turtles, whales, and bumphead sunfish (*Mola alexandrini*) have been shown to have ocean current-assisted migration (Gaspar et al. 2006; Shillinger et al. 2008; Tyson Moore et al. 2020; Chang et al. 2021). Supporting this migration assistance hypothesis is our finding that the center of gravity for age-2 hake had the strongest correlation with mean annual northward velocity (Table 3), suggesting the youngest and smallest hake tend to be distributed further north in years with a stronger northward flowing undercurrent.

These two hypotheses, however, are not mutually exclusive and could have different relative importance across age groups. For example, different relative importances between younger and older age groups may be driven by ontogenetic changes in diet. Hake diets tend to become more piscivorous with increasing age and size (Livingston and Bailey 1985; Buckley and Livingston 1997). Consequently, prey for older hake may be less impacted by changes in the undercurrent due to being more active swimmers compared to prey items for younger hake. Alternatively, the vertical distribution of hake in the water column may vary by age. For instance, younger hake may be shallower in the water column, possibly due to smaller prey being more surface oriented during certain parts of the day (Nielson and Perry 1990; Tanasichuk et al. 1991; Pillar and Barange 1995). Understanding how the CU impacts the distribution of key hake diet items, e.g., euphausiids, would be a useful next step in determining the mechanisms underpinning the spatial and ontogenetic varying relationships observed here.

The functional form and complexity of the relationships between hake distribution and the CU reported here differed from those previously reported. In particular, Agostini et al. (2008) found a spatially stationary dome-shaped relationship between hake density and the strength of the undercurrent with the strongest effect occurring at velocities around 0.4 m·s^{-1}. This relationship, however, was estimated using data from only 1995 and 1998 and a limited geographic range (38–43°N). The expanded spatial extent and temporal period of this study likely explain why we found

more complex relationships between hake distribution and the CU. For instance, the spatial range analyzed in Agostini et al. (2008) corresponds to the region where we found a cross-shelf gradient in the undercurrent effects, but excludes more northern areas where the undercurrent tended to be weaker and have more spatially consistent effects on hake distribution.

Our results indicate that in the northern part of the study region (44–48.3°N), when there is a stronger northward current there is a lower probability of finding hake, but if hake are found there tends to be more of them at a given location. For example, in 2009 the undercurrent had the highest average northward velocity in the region north of 44°N, as well as a high percent hake absent rate (78%), but the highest average hake densities in places where hake were present (1808 t). One possible explanation for this pattern is that in this northern region, hake may aggregate in locations with a stronger undercurrent, resulting in a patchier distribution. Santora et al. (2018) showed that euphausiids, a key hake prey item, tend to aggregate near submarine canyons. These submarine canyons provide bathymetric complexity that may interact with undercurrent flow patterns and eddy formation causing prey to aggregate in these areas (Foreman et al. 2008; Thomson and Krassovski 2010). Similarly, Malick et al. (2020b) showed that hake tend to be found just offshore of the 200 m shelf break in this northern region, most likely due to preferences of euphausiids to concentrate in shelf-break areas (Santora et al. 2012, 2018; Phillips et al. 2022).

In more southern areas, we found a synchronous cross-shelf gradient in the undercurrent effects for the occurrence and density models. In particular, a stronger northward flow resulted in higher (lower) probabilities of finding hake and higher (lower) densities in nearshore (offshore) areas. This cross-shelf gradient was also observed for the older hake densities. Similar to the more northern pattern, this cross-shelf distribution pattern may be driven by prey availability. In particular, the two highest years of northward flow, 2009 and 2017, are also years where large euphausiid aggregations were present in nearshore areas south of 44°N; in 2009, euphausiids were aggregated near Cape Mendocino and in 2017 they were aggregated near Cape Blanco (Phillips et al. 2022, 2023).

Our finding that the average northward flow was 2.2 times higher in the region south of 44°N compared to more northern areas is consistent with several previous studies and may be driven by changes in the oceanographic drivers of the northward flow (Garfield et al. 1999; Pierce et al. 2000; Agostini et al. 2006). Indeed, Connolly et al. (2014) used ocean circulation models and found a transition in the drivers of the undercurrent occurred near Cape Blanco (42°N); north of this transition, the undercurrent was forced by alongshore density gradients, not a northward sloping sea surface. We also found that the undercurrent in the region south of 44°N exhibited a cross-shelf gradient with northward flows highest on the slope (Fig. S2), which is consistent with findings that the core of the undercurrent tends to be near the shelf slope in the region 35°N and 42.2°N (Pierce et al. 2000; Kurapov et al. 2017).

In this study, we only evaluated the north–south velocity of the undercurrent and how it is associated with hake distribution. Subsurface horizontal ocean movement, however, can also have a strong cross-shelf component that can vary at meso- and sub-mesoscales. In the CCE, underwater eddies associated with the undercurrent (known as cuddies) provide areas of complex horizontal movement (Garfield et al. 1999; Kurian et al. 2011). These subsurface eddies generally travel from nearshore to offshore, providing cross-shelf lateral movement that can have unique oceanographic characteristics, including temperature and salinity (Collins et al. 2013; Pelland et al. 2013; McWilliams 2019). Eddies have been widely shown to have positive associations with pelagic fish distribution, most likely by providing highly productive pockets within an otherwise weakly structured environment (Brandt 1981; Godø et al. 2012). Given the importance of eddies to structuring pelagic environments, we suggest research directed at understanding the ecology of subsurface eddies associated with the CU as a fruitful avenue for future work.

Although the northern extent of our study region was 48.3°N (due to limited survey undercurrent data in more northern areas), the CU has been shown to carry water as far north and west as the Aleutian Islands (Thomson and Krassovski 2010). Hake distribution extends into Alaska waters in some years (e.g., 1998) indicating, that the undercurrent may also have impacts on hake distribution in areas north of those examined in this study. In particular, relationships between the undercurrent and hake distribution along the West Coast of Vancouver Island may be important, as this area is thought to be an important area that aggregates hake prey due to complex bathymetry (Mackas et al. 1997, 2001). In addition, 2009 and 2017, the two years with the highest average northward velocity, had comparatively high proportions of hake biomass in Canadian waters (Berger et al. 2023), providing a first indication that the undercurrent may impact biomass distribution across the U.S. and Canada border and the subsequent management of transboundary hake fishery.

In conclusion, our results provide further evidence that hake distribution has spatially and ontogenetically heterogeneous responses to environmental variability. Increasing our capacity to anticipate responses of ecologically important species is a pressing concern as the climate warms and shifts in mean ocean conditions emerge from the historical envelope (Henson et al. 2017; Dietze et al. 2018). Our results suggest that future impacts of climate change on hake are likely to have spatially complex effects that are conditioned on the age-structure of the population (Meinvielle and Johnson 2013). This spatial and ontogenetic non-stationarity further suggests that short-term forecasts are a promising avenue to anticipating impacts of environmental variability on hake that can provide timely information to stakeholders (e.g., fishers) and managers (Malick et al. 2020*b*). Indeed, our results indicate that extending existing tools used to inform management of hake, such as seasonal habitat forecasts and management strategy evaluations (Malick et al. 2020*b*; Jacobsen et al. 2022), to include undercurrent dynamics may help to better resolve future changes in hake distribution.

Acknowledgements

We thank Rebecca Thomas and Dezhang Chu for assistance with the hake biomass data, as well as for helpful discussions that improved this study. We also thank Julia Hummon for helpful discussions about the undercurrent data. Thanks to Isaac Kaplan, Kiva Oken, Nick Bond, and an anonymous reviewer for useful comments and discussion about the manuscript. We are thankful to the captains and crew members of the vessels used to conduct the acoustic-trawl surveys.

Article information

History dates

Received: 18 July 2023
Accepted: 3 October 2023
Accepted manuscript online: 18 October 2023
Version of record online: 12 December 2023

Data availability

Data generated or analyzed during this study are available from the corresponding author upon reasonable request.

Author information

Author ORCIDs

Michael J. Malick https://orcid.org/0000-0002-8376-5476
Mary E. Hunsicker https://orcid.org/0000-0002-3036-1515
Melissa A. Haltuch https://orcid.org/0000-0003-2821-1267
Kristin N. Marshall https://orcid.org/0000-0002-9769-2300
Aaron M. Berger https://orcid.org/0000-0002-1408-7122
Samantha A. Siedlecki https://orcid.org/0000-0002-5662-7326
Stéphane Gauthier https://orcid.org/0009-0000-3514-765X
Albert J. Hermann https://orcid.org/0000-0002-0253-7464

Author contributions

Conceptualization: MJM, MEH, MAH, SLP, KNM, AMB, SAS, SG, AJH
Data curation: SLP, JEP, SG
Formal analysis: MJM
Funding acquisition: MEH
Methodology: MJM, MEH, MAH, SLP, KNM, AMB, SAS
Writing – original draft: MJM, JEP
Writing – review & editing: MJM, MEH, MAH, SLP, KNM, JEP, AMB, SAS, SG, AJH

Competing interests

The authors declare there are no competing interests.

Funding information

Partial funding was provided by NOAA's Fisheries and the Environment (FATE) program (grant No. 16-08).

Supplementary material

Supplementary data are available with the article at https://doi.org/10.1139/cjfas-2023-0202.

References

Agostini, V.N., Francis, R.C., Hollowed, A.B., Pierce, S.D., Wilson, C., and Hendrix, A.N. 2006. The relationship between Pacific hake (*Merluccius productus*) distribution and poleward subsurface flow in the California Current System. Can. J. Fish. Aquat. Sci. **63**: 2648–2659. doi:10.1139/f06-139.

Agostini, V.N., Hendrix, A.N., Hollowed, A.B., Wilson, C.D., Pierce, S.D., and Francis, R.C. 2008. Climate–ocean variability and Pacific hake: a geostatistical modeling approach. J. Mar. Syst. **71**: 237–248. doi:10.1016/j.jmarsys.2007.01.010.

Bakun, A. 1996. Patterns in the ocean: ocean processes and marine population dynamics. California Sea Grant College System, NOAA.

Berger, A.M., Grandin, C.J., Johnson, K.F., and Edwards, A.M. 2023. Status of the Pacific hake (whiting) stock in the U.S. and Canadian waters in 2023. Prepared by the Joint Technical Committee for Pacific Hake/Whiting Agreement, National Marine Fisheries Service and Fisheries and Oceans Canada. 208p.

Brandt, S.B. 1981. Effects of a warm-core eddy on fish distributions in the Tasman Sea off east Australia. Mar. Ecol. Prog. Ser. **6**: 19–33. doi:10.3354/meps006019.

Brodie, S., Thorson, J.T., Carroll, G., Hazen, E.L., Bograd, S., Haltuch, M.A., et al. 2019. Trade-offs in covariate selection for species distribution models: a methodological comparison. Ecography, **43**: 11–24. doi:10.1111/ecog.04707.

Buckley, T.W., and Livingston, P.A. 1997. Geographic variation in the diet of Pacific hake, with a note on cannibalism. Cal. Coop. Ocean. Fish. **28**: 53–62.

Chang, C.-T., Chiang, W.-C., Musyl, M.K., Popp, B.N., Lam, C.H., Lin, S.-J., et al. 2021. Water column structure influences long-distance latitudinal migration patterns and habitat use of bumphead sunfish *Mola alexandrini* in the Pacific Ocean. Sci. Rep. **11**: 21934. doi:10.1038/s41598-021-01110-y. PMID: 34753959.

Ciannelli, L., Bartolino, V., and Chan, K.-S. 2012. Non-additive and non-stationary properties in the spatial distribution of a large marine fish population. Proc. R. Soc. B, **279**: 3635–3642. doi:10.1098/rspb.2012.0849.

Collins, C.A., Margolina, T., Rago, T.A., and Ivanov, L. 2013. Looping RAFOS floats in the California Current System. Deep Sea Res. Part II, **85**: 42–61. doi:10.1016/j.dsr2.2012.07.027.

Connolly, T.P., Hickey, B.M., Shulman, I., and Thomson, R.E. 2014. Coastal trapped waves, alongshore pressure gradients, and the California Undercurrent. J. Phys. Oceanogr. **44**: 319–342. doi:10.1175/JPO-D-13-095.1.

Di Lorenzo, E., Combes, V., Keister, J.E., Strub, P.T., Thomas, A.C., Franks, P.J.S., et al. 2013. Synthesis of Pacific Ocean climate and ecosystem dynamics. Oceanography, **26**: 68–81. doi:10.5670/oceanog.2013.76.

Dietze, M.C., Fox, A., Beck-Johnson, L.M., Betancourt, J.L., Hooten, M.B., Jarnevich, C.S., et al. 2018. Iterative near-term ecological forecasting: needs, opportunities, and challenges. Proc. Natl. Acad. Sci. U.S.A. **115**: 1424–1432. doi:10.1073/pnas.1710231115.

Fleischer, G.W., Cooke, K.D., Ressler, P.H., Thomas, R.E., de Blois, S.K., and Hufnagle, L.C. 2008. The 2005 integrated acoustic and trawl survey of Pacific hake, *Merluccius productus*. *In* U.S. and Canadian waters off the Pacific coast. Tech. Memo. NMFS-NWFSC-94. National Oceanic & Atmospheric Administration, Seattle, WA.

Foreman, M.G.G., Callendar, W., MacFadyen, A., Hickey, B.M., Thomson, R.E., and Di Lorenzo, E. 2008. Modeling the generation of the Juan de Fuca Eddy. J. Geophys. Res. **113**: C03006. doi:10.1029/2006JC004082.

Garfield, N., Collins, C.A., Paquette, R.G., and Carter, E. 1999. Lagrangian exploration of the California Undercurrent, 1992. J. Phys. Oceanogr. **29**: 560–583. doi:10.1175/1520-0485(1999)029⟨0560:LEOTCU⟩2.0.CO;2.

Gaspar, P., Georges, J.-Y., Fossette, S., Lenoble, A., Ferraroli, S., and Le Maho, Y. 2006. Marine animal behaviour: neglecting ocean currents can lead us up the wrong track. Proc. R. Soc. B, **273**: 2697–2702. doi:10.1098/rspb.2006.3623.

Godø, O.R., Samuelsen, A., Macaulay, G.J., Patel, R., Hjøllo, S.S., Horne, J., et al. 2012. Mesoscale eddies are oases for higher trophic marine life. PLoS One, **7**: e30161. doi:10.1371/journal.pone.0030161.

Henson, S.A., Beaulieu, C., Ilyina, T., John, J.G., Long, M., Séférian, R., et al. 2017. Rapid emergence of climate change in environmental drivers of marine ecosystems. Nat. Commun. **8**: 14682. doi:10.1038/ncomms14682.

Hickey, B.M., and Banas, N.S. 2008. Why is the northern end of the California Current System so productive? Oceanography, **21**: 90–107. doi:10.5670/oceanog.2008.07.

Jacobsen, N.S., Marshall, K.N., Berger, A.M., Grandin, C., and Taylor, I.G. 2022. Climate-mediated stock redistribution causes increased risk and challenges for fisheries management. ICES J. Mar. Sci. **79**: 1120–1132. doi:10.1093/icesjms/fsac029.

Keister, J.E., Di Lorenzo, E., Morgan, C.A., Combes, V., and Peterson, W.T. 2011. Zooplankton species composition is linked to ocean transport in the Northern California Current. Global Change Biol. **17**: 2498–2511. doi:10.1111/j.1365-2486.2010.02383.x.

Kurapov, A.L., Pelland, N.A., and Rudnick, D.L. 2017. Seasonal and interannual variability in along-slope oceanic properties off the US West Coast: inferences from a high-resolution regional model. J. Geophys. Res. Oceans, **122**: 5237–5259. doi:10.1002/2017JC012721.

Kurian, J., Colas, F., Capet, X., McWilliams, J.C., and Chelton, D.B. 2011. Eddy properties in the California Current System. J. Geophys. Res. **116**: C08027. doi:10.1029/2010JC006895.

Laufkötter, C., Zscheischler, J., and Frölicher, T.L. 2020. High-impact marine heatwaves attributable to human-induced global warming. Science, **369**: 1621–1625. doi:10.1126/science.aba0690.

Li, Z., Ye, Z., Wan, R., Tanaka, K.R., Boenish, R., and Chen, Y. 2018. Density-independent and density-dependent factors affecting spatiotemporal dynamics of Atlantic cod (*Gadus morhua*) distribution in the Gulf of Maine. ICES J. Mar. Sci. **75**: 1329–1340. doi:10.1093/icesjms/fsx246.

Livingston, P.A., and Bailey, K.M. 1985. Trophic role of the Pacific whiting, *Merluccius productus*. Mar. Fish. Rev. **47**: 16–22.

Mackas, D.L., Kieser, R., Saunders, M., Yelland, D.R., Brown, R.M., and F., M.D. 1997. Aggregation of euphausiids and Pacific hake (*Merluccius productus*) along the outer continental shelf off Vancouver Island. Can. J. Fish. Aquat. Sci. **54**: 2080–2096. doi:10.1139/cjfas-54-9-2080.

Mackas, D.L., Thomson, R.E., and Galbraith, M. 2001. Changes in the zooplankton community of the British Columbia continental margin, 1985, and their covariation with oceanographic conditions. Can. J. Fish. Aquat. Sci. **58**: 685–702. doi:10.1139/f01-009.

Malick, M.J., Cox, S.P., Mueter, F.J., Dorner, B., and Peterman, R.M. 2017. Effects of the North Pacific Current on the productivity of 163 Pacific salmon stocks. Fish. Oceanogr. **26**: 268–281. doi:10.1111/fog.12190.

Malick, M.J., Hunsicker, M.E., Haltuch, M.A., Parker-Stetter, S.L., Berger, A.M., and Marshall, K.N. 2020*a*. Relationships between temperature and Pacific hake distribution vary across latitude and life-history stage. Mar. Ecol. Prog. Ser. **639**: 185–197. doi:10.3354/meps13286.

Malick, M.J., Siedlecki, S.A., Norton, E.L., Kaplan, I.C., Haltuch, M.A., Hunsicker, M.E., et al. 2020*b*. Environmentally driven seasonal forecasts of Pacific hake distribution. Front. Mar. Sci. **7**: 578490. doi:10.3389/fmars.2020.578490.

McWilliams, J.C. 2019. A survey of submesoscale currents. Geosci. Lett. **6**: 3. doi:10.1186/s40562-019-0133-3.

Meinvielle, M., and Johnson, G.C. 2013. Decadal water-property trends in the California Undercurrent, with implications for ocean acidification: trends in the California Undercurrent. J. Geophys. Res. Oceans, **118**: 6687–6703. doi:10.1002/2013JC009299.

Miller, T.W., Brodeur, R.D., Rau, G., and Omori, K. 2010. Prey dominance shapes trophic structure of the northern California Current pelagic food web: evidence from stable isotopes and diet analysis. Mar. Ecol. Prog. Ser. **420**: 15–26. doi:10.3354/meps08876.

Nielson, J.D., and Perry, R.I. 1990. Diel vertical migrations of marine fishes: an obligate or facultative process? Adv. Mar. Biol. **26**: 115–168. doi:10.1016/S0065-2881(08)60200-X.

NOAA. 2017. Fisheries economics of the United States, 2015. Tech. Memo. NMFS-F/SPO-170, 247. National Oceanic & Atmospheric Administration. Available from http://www.st.nmfs.noaa.gov/economics/publications/feus/fisheries_economics_2015/index [accessed 19 December 2022].

Pelland, N.A., Eriksen, C.C., and Lee, C.M. 2013. Subthermocline eddies over the Washington continental slope as observed by seagliders, 2003. J. Phys. Oceanogr. **43**: 2025–2053. doi:10.1175/JPO-D-12-086.1.

Peterson, W.T., and Keister, J.E. 2003. Interannual variability in copepod community composition at a coastal station in the northern California Current: a multivariate approach. Deep Sea Res. Part II, **50**: 2499–2517. doi:10.1016/S0967-0645(03)00130-9.

Phillips, E.M., Chu, D., Gauthier, S., Parker-Stetter, S.L., Shelton, A.O., and Thomas, R.E. 2022. Spatiotemporal variability of euphausiids in the California Current Ecosystem: insights from a recently developed time series. ICES J. Mar. Sci. **79**: 1312–1326. doi:10.1093/icesjms/fsac055.

Phillips, E.M., Malick, M.J., Gauthier, S., Haltuch, M.A., Hunsicker, M.E., Parker-Stetter, S.L., and Thomas, R.E. 2023. The influence of temperature on Pacific hake co-occurrence with euphausiids in the California Current Ecosystem. Fish. Oceanogr. **32**: 267–279. doi:10.1111/fog.12628.

Pierce, S.D., Smith, R.L., Kosro, P.M., Barth, J.A., and Wilson, C.D. 2000. Continuity of the poleward undercurrent along the eastern boundary of the mid-latitude north Pacific. Deep Sea Res. Part II, **47**: 811–829. doi:10.1016/s0967-0645(99)00128-9.

Pillar, S.C., and Barange, M. 1995. Diel feeding periodicity, daily ration and vertical migration of juvenile Cape hake off the west coast of South Africa. J. Fish Biol. **47**: 753–768. doi:10.1111/j.1095-8649.1995.tb06000.x.

Pinsky, M.L., Reygondeau, G., Caddell, R., Palacios-Abrantes, J., Spijkers, J., and Cheung, W.W.L. 2018. Preparing ocean governance for species on the move. Science, **360**: 1189–1191. doi:10.1126/science.aat2360.

R Core Team. 2019. R: a language and environment for statistical computing. R Foundation for Statistical Computing, Vienna, Austria.

Ressler, P.H., Holmes, J.A., Fleischer, G.W., Thomas, R.E., and Cooke, C.K. 2007. Pacific hake, *Merluccius productus*, autecology: a timely review. Mar. Fish. Rev. **69**: 1–24.

Rykaczewski, R.R., and Checkley, D.M. 2008. Influence of ocean winds on the pelagic ecosystem in upwelling regions. Proc. Natl. Acad. Sci. U.S.A. **105**: 1965–1970. doi:10.1073/pnas.0711777105.

Santora, J.A., Sydeman, W.J., Schroeder, I.D., Wells, B.K., and Field, J.C. 2011. Mesoscale structure and oceanographic determinants of krill hotspots in the California Current: implications for trophic transfer and conservation. Prog. Oceanogr. **91**: 397–409. doi:10.1016/j.pocean.2011.04.002.

Santora, J.A., Sydeman, W.J., Schroeder, I.D., Reiss, C.S., Wells, B.K., Field, J.C., et al. 2012. Krill space: a comparative assessment of mesoscale structuring in polar and temperate marine ecosystems. ICES J. Mar. Sci. **69**: 1317–1327. doi:10.1093/icesjms/fss048.

Santora, J.A., Zeno, R., Dorman, J.G., and Sydeman, W.J. 2018. Submarine canyons represent an essential habitat network for krill hotspots in a large marine ecosystem. Sci. Rep. **8**: 7579. doi:10.1038/s41598-018-25742-9.

Shillinger, G.L., Palacios, D.M., Bailey, H., Bograd, S.J., Swithenbank, A.M., Gaspar, P., et al. 2008. Persistent leatherback turtle migrations present opportunities for conservation. PLoS Biol. **6**: e171. doi:10.1371/journal.pbio.0060171.

Tanasichuk, R.W., Ware, D.M., Shaw, W., and McFarlane, G.A. 1991. Variations in diet, daily ration, and feeding periodicity of Pacific hake (*Merluccius productus*) and spiny dogfish (*Squalus acanthias*) off the lower west coast of Vancouver Island. Can. J. Fish. Aquat. Sci. **48**: 2118–2128. doi:10.1139/f91-251.

Thomson, R.E., and Krassovski, M.V. 2010. Poleward reach of the California Undercurrent extension. J. Geophys. Res. **115**: C09027. doi:10.1029/2010JC006280.

Thomson, R.E., and Krassovski, M.V. 2015. Remote alongshore winds drive variability of the California Undercurrent off the British Columbia-Washington coast. J. Geophys. Res. Oceans, **120**: 8151–8176. doi:10.1002/2015JC011306.

Tyson Moore, R.B., Douglas, D.C., Nollens, H.H., Croft, L., and Wells, R.S. 2020. Post-release monitoring of a stranded and rehabilitated short-finned pilot whale (*Globicephala macrorhynchus*) reveals current-assisted travel. Aquat Mamm. **46**: 200–214. doi:10.1578/AM.46.2.2020.200.

Wood, S.N. 2003. Thin plate regression splines. J. R. Stat. Soc. B, **65**: 95–114. doi:10.1111/1467-9868.00374.

Wood, S.N. 2011. Fast stable restricted maximum likelihood and marginal likelihood estimation of semiparametric generalized linear models. J. R. Stat. Soc. B, **73**: 3–36. doi:10.1111/j.1467-9868.2010.00749.x.

Wood, S.N. 2017. Generalized additive models: an introduction with R. CRC Press, Boca Raton, FL.